SUPPLEMENTARY INFORMATION

High-flux and high-resolution coded-source radiography based on picosecond laser-irradiated tube targets

Meng-Ting Li,[1,2] Tian-Kui Zhang,[1] Ming-Hai Yu,[1] Yao-Xiang Song,[1] Zi-Tao Wang,[1] Yong-Hong Yan,[1] Fang Tan,[1] Lei Yang,[1] Feng Lu,[1] Shao-Yi Wang,[1] Kai-Nan Zhou,[1] Wei-Min Zhou,[1,3] Zong-Qing Zhao[1] and Yu-Qiu Gu[1,4,5,*]

[1] *Science and Technology on Plasma Physics Laboratory, Laser Fusion Research Center, China Academy of Engineering Physics, Mianyang 621900, China*
[2] *School of Physical Science and Technology, Xinjiang University, Urumqi 830017, China*
[3] *IFSA Collaborative Innovation Center, Shanghai Jiao Tong University, Shanghai 200240, China*
[4] *Shanghai Institute of Laser Plasma, China Academy of Engineering Physics, Shanghai 201899, China*
[5] *Center for Advanced Material Diagnostic Technology, Shenzhen Technology University, Shenzhen, China*

SUPPLEMENTARY NOTE 1: RESULTS OF THE MEDIUM-TUBE TARGET

The medium-tube targets were fabricated via sputter deposition method. It is challenging to maintain a constant wall thickness for a tube. The removal of the central quartz substrate was also difficult. The cutting process can also cause deformation and stretching of the gold material. All these factors contribute to an inferior quality of the finished medium-diameter targets. Supplementary Figure 1(a) and (b) show the end face of a medium-tube target and the X-ray source it generates. Due to the unevenness in wall thickness, the X-ray source has a crescent-shaped distribution, with the annulus width varying significantly from 0 to over 10 μm. Owing to the randomness and irregularity in the source shape, the blind method we employed for image reconstruction is ineffective for the medium-tube target.

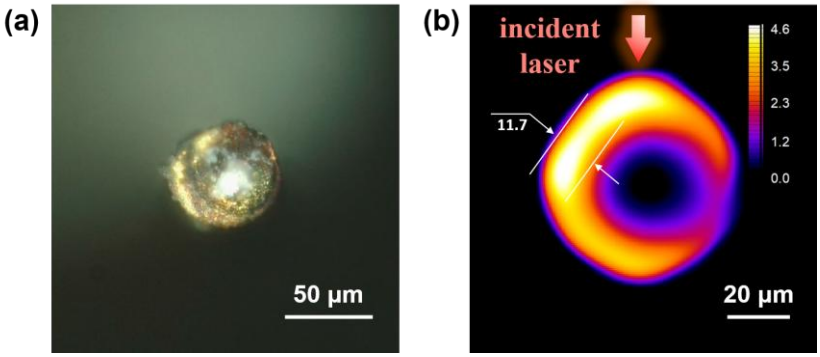

Supplementary Figure 1. Medium-tube target and the formed X-ray source. (a) Microscope image of the end face of a medium-tube target. (b) Two-dimension intensity distribution of the annular X-ray source using a medium-tube target. The red arrow indicates the position of incident laser.

Additionally, the target is not a perfect hollow structure, as the quartz material remains in the center. It transfers hot-electron energy into a colder bremsstrahlung channel, leading a lower radiation temperature and consequently lower $CE_{50\text{-}200}$, as mentioned in the main context.

SUPPLEMENTARY NOTE 2: RESULTS OF A NON-UNIFORM ANNULAR SOURCE

The resolution lines were reconstructed using blind deconvolution algorithm[1,2] which alternatively corrects both the system's point spread function (PSF) and the resulting image, mitigating the effects of the source variation to some extent. After deconvolution, PSF will evolve from the preset shape into a function that reflect the true X-ray source.

Supplementary Figure 2(a) shows an annular X-ray source produced using a large-tube target. The intensity distribution is highly non-uniform, which is significantly inferior to the results from other large tubes. This anomaly, along with a very low radiation intensity, may be attributed to a laser output failure or other unforeseen factors. However, the images of resolution lines can be successfully recovered, displaying a clearly identifiable structure. Supplementary Figure 2(b) presents the reconstruction results of the horizontal resolution lines with a 40 μm period. The corresponding PSF evolves from the preset uniform annulus (Supplementary Figure 2(c)) into a non-uniform distribution (Supplementary Figure 2(d)), with its brightest region at the bottom. This spatial pattern is consistent with the measured source distribution in (a).

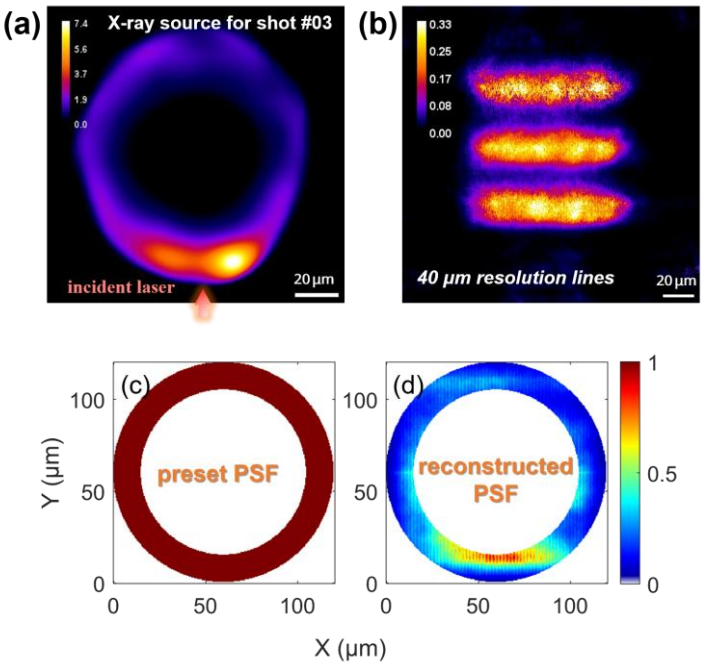

Supplementary Figure 2. Results of a highly non-uniform X-ray source. (a) Two-dimension intensity distribution of the highly non-uniform X-ray source using a large-tube target. The red arrow indicates the position of incident laser. (b) Reconstructed images of the 40 μm-period horizontal resolution lines for coded-source radiography with the X-ray source from (a). (c) Preset and (d) reconstructed point spread function (PSF) in the reconstruction of (b) using blind deconvolution.

This result demonstrates the algorithm's capability to partially compensate for the imperfections in the X-ray source and produce reliable reconstructed images. Nevertheless, a uniform annular X-ray source is still crucial for successful imaging. In this case, the centroid of the source was displaced from the designed radiography axis, resulting in more pronounced image distortion compared to other radiography.

REFERENCES

1 Levin, A., Weiss, Y., Durand, F. & Freeman, W. T. in *2009 IEEE Conference on Computer Vision and Pattern Recognition*. 1964-1971.

2 He, W. H. *et al.* Blind deconvolution for spatial distribution of Kα emission from ultraintense laser-plasma interaction. *Optics Express* **22**, 5875-5882 (2014).